Temperature response measurements from eucalypts give insight into the impact of Australian isoprene emissions on air quality in 2050

Kathryn M. Emmerson[1], Malcolm Possell[2], Michael J. Aspinwall[3,4], Sebastian Pfautsch[3], and Mark G. Tjoelker[3]

[1]Climate Science Centre, CSIRO Oceans and Atmosphere, Aspendale, VIC 3195 Australia
[2]School of Life and Environmental Sciences, University of Sydney, Sydney, NSW, Australia
[3]Hawkesbury Institute for the Environment, Western Sydney University, Penrith, NSW, Australia
[4]Department of Biology, University of North Florida, Jacksonville, Florida, 32224 USA

Correspondence: Kathryn Emmerson (kathryn.emmerson@csiro.au)

Abstract. Predicting future air quality in Australian cities dominated by eucalypt emissions requires an understanding of their emission potentials in a warmer climate. Here we measure the temperature response in isoprene emissions from saplings of four different *Eucalyptus* species grown under current and future average summertime temperature conditions. The future conditions represent a 2050 climate under Representative Concentration Pathway 8.5, with average daytime temperatures of 294.5 K. Ramping the temperature from 293 K to 328 K resulted in these eucalypts emitting isoprene at temperatures 4-9 K higher than default maximum emission temperature in the Model of Emissions of Gases and Aerosols from Nature (MEGAN). New basal emission rate measurements were obtained at the standard conditions of 303 K leaf temperature and 1000 μmol m^{-2} s^{-1} photosynthetically active radiation and converted into landscape emission factors. We applied the eucalypt temperature responses and emission factors to Australian trees within MEGAN and ran the CSIRO Chemical Transport Model for three summertime campaigns in Australia. Compared to the default model, the new temperature responses resulted in less isoprene emission in the morning and more during hot afternoons, improving the statistical fit of modelled to observed ambient isoprene. Compared to current conditions, an additional 2 ppb of isoprene is predicted in 2050 causing hourly increases up to 21 ppb of ozone and 24-hourly increases of 0.4 μg m^{-3} of aerosol in Sydney. A 550 ppm CO_2 atmosphere in 2050 mitigates these peak Sydney ozone mixing ratios by 4 ppb. Nevertheless, these forecasted increases in ozone are up to one fifth of the hourly Australian air quality limit and suggests anthropogenic NO_X should be further reduced to maintain healthy air quality in future.

1 Introduction

Biogenic volatile organic compounds (BVOCs) are emitted by vegetation in response to external stressors such as heat, light and herbivory (Sharkey and Monson, 2017). There are hundreds of individual BVOCs all exhibiting different emission behaviours

(e.g. with or without a light dependence), but the largest global flux of a single BVOC is isoprene (2-methyl-1,3-butadiene; C_5H_8), with an estimated 440 - 600 Tg C per year (Guenther et al., 2012). Isoprene reacts rapidly in the atmosphere, contributing to ozone (O_3) and secondary organic aerosol (SOA) formation. For cities surrounded by forests, BVOC emissions can dominate airsheds contributing to peak summertime ozone (Utembe et al., 2018), and early morning ozone spikes (Millet et al., 2016) if not quenched by the hydroxyl radical (OH) on the previous day.

In addition to the different environmental reasons a plant will emit BVOCs, plants emit their own unique signature of BVOCs with varying strengths, even amongst plants in the same genus. Native to Australia, eucalypt trees are amongst the highest BVOC emitters of any plant species (Evans et al., 1982; Benjamin et al., 1996; Kesselmeier and Staudt, 1999), emitting isoprene constitutively and storing monoterpenes within oil reservoirs in the leaves (Brophy et al., 1991). However, very few of the 800 species in the *Eucalyptus* genus (Department of Agriculture and Water Resources, 2018) have been studied for emissions. This is problematic as biogenic modellers tend to base simulations on a few measurements which represent a fraction of the potential diversity of species and emission rates. For example, the *Eucalyptus* isoprene emission factors for the Model of Emissions of Gases and Aerosols from Nature (MEGAN) were based on six studies, only one of which was conducted in Australia (see Emmerson et al. (2016)). The Australian study measured large differences of 63 μg g^{-1} h^{-1} of isoprene between the lowest and highest emitting eucalypt species, with *E. globulus* showing the greatest emission rates (He et al., 2000). Natural occurrence of *E. globulus* is restricted to temperate south east Australia (including Tasmania).

Use of landscape emission factors (LEF) weighted by higher emitting trees have caused overpredictions in modelled isoprene (Emmerson et al., 2016, 2019a). As young leaves tend to emit more isoprene than older leaves, conducting emission measurements on saplings has been questioned (Street et al., 1997), although adult trees will contain a mixture of leaf ages. However, BVOC emission models such as MEGAN require isoprene emission rates to be determined at standard conditions of 303 K and 1000 μmol m^{-2} s^{-1} photosynthetically active radiation (PAR) (Guenther et al., 2012). Measurements made at other temperatures and PAR fluxes need scaling to these standard conditions, which can introduce uncertainties of up to 20 % (He et al., 2000). The standard temperature and light level conditions are better provided for in a controlled greenhouse environment, which necessitates using saplings.

MEGAN describes the emission of BVOCs in terms of temperature, PAR, leaf area index, leaf age, soil moisture, and suppression via ambient CO_2 concentrations. Whilst the MEGAN parameterisations are fitted from a wide range of ecosystem responses to environmental conditions, there are spatial and temporal exceptions to these standards which are comprehensively reviewed by Niinemets et al. (2010). Many studies have investigated impacts of climate change on isoprene by changing the inputs to MEGAN such as ambient temperatures and CO_2 concentrations (e.g. Bauwens et al. (2018), and how land use might change the geographical extent of plant functional types (PFTs) (e.g. Arneth et al. (2011)), without changing the MEGAN parameterisations themselves. Here we report new controlled isoprene response measurements from four eucalypt tree species, which show different temperature responses than assumed by MEGAN. We also use the controlled experimental conditions to impose a projected 2050 climate to investigate whether eucalypts growing in a warmer climate show a different temperature sensitivity of isoprene emissions than eucalypts growing in the current climate. Accounting for climate warming impacts on isoprene emission capacity provides a lens to study how air quality in Australia could be impacted in the future. Using a

regional chemical transport model allows us to alter the dynamics of MEGAN to suit these new temperature responses for Australia.

This study aims to i) determine the temperature response of isoprene in four Eucalyptus species grown under two treatments representing current average summertime temperatures and a 2050 climate, and ii) use these measurements to determine the impacts of isoprene in a future climate on predicted levels of O_3 and SOA.

2 Methods

2.1 The MEGAN default temperature response

Guenther et al. (2012) defines the emission of BVOCs in terms of activity factors representing the environmental conditions described above. Here we are interested in studying the temperature response of isoprene, γT (unitless):

$$\gamma T = E_{\mathrm{opt}} \times \left[\frac{C_{\mathrm{T2}} \times exp(C_{\mathrm{T1}} \times x)}{(C_{\mathrm{T2}} - C_{\mathrm{T1}} \times (1 - exp(C_{\mathrm{T2}} \times x)))} \right] \quad (1)$$

where E_{opt} is the optimum emission point, and C_{T1} (95 kJ mol^{-1}) and C_{T2} (230 kJ mol^{-1}) are coefficients that fit the response to a range of ecosystems.

$$x = \left[\frac{(1/T_{\mathrm{opt}}) - (1/T)}{0.00831} \right] \quad (2)$$

where T is the temperature of the leaf (K) and 0.00831 is the gas constant in kJ K^{-1} mol^{-1}. The optimum temperature for emission in MEGAN, T_{opt} is calculated below.

$$T_{\mathrm{opt}} = T_{\mathrm{max}} + (0.6 \times (T_{240} - T_{\mathrm{S}})) \quad (3)$$

$$E_{\mathrm{opt}} = C_{\mathrm{eo}} \times exp(0.05 \times (T_{24} - T_{\mathrm{S}})) \times exp(0.05 \times (T_{240} - T_{\mathrm{S}})) \quad (4)$$

where T_{max} is 313 K, T_s is the standard leaf temperature (297 K), and T_{24} and T_{240} are the average leaf temperatures of the previous 24 and 240 hours, respectively. C_{eo} is an empirical coefficient of 2 for isoprene.

2.2 Experimental conditions

Four eucalypt species were chosen based on their prevalence in Australia, and in particular New South Wales (Table 1). *E. camaldulensis* and *E. tereticornis* have a wide geographical representation within Australia, with a latitudinal native growing range of 9-38 °S (Atlas of Living Australia, 2019) (supplementary figure S1). *E. camaldulensis* is the most widely naturally distributed species of all eucalypts in Australia (Atlas of Living Australia, 2019). The native climatic distribution range of *E. botryoides* and *E. smithii* are restricted to the south east coastal regions. All four species are forecast to exist in future, but only *E. camaldulensis* is predicted to expand its growing area by 2085 (González-Orozco et al., 2016).

Plant species can be classified as low (less than 1 μg g^{-1} h^{-1}), moderate (1-10 μg g^{-1} h^{-1}) or high (greater than 10 μg g^{-1} h^{-1}) isoprene emitters (Benjamin et al., 1996). Of the four eucalypts used in this study, *E. camaldulensis* and *E. tereticornis* are high

isoprene emitters (Table 1), whilst *E. botryoides* is classed as moderate. The emission category of *E. smithii* is unknown. All tabulated measurements were scaled to the standard conditions from other temperatures and PAR.

Eighty trees (20 of each species) were grown from seed at Hawkesbury Institute for the Environment in Richmond, NSW. After eight weeks seedlings were transplanted into 6.9 L pots filled with alluvial soil and split randomly into two treatment groups, each containing 10 seedlings of each species. The first treatment group was grown for 85 days at an average daily temperature of 291 K (current climate) and the second treatment group was grown for 85 days at 294.5 K (future climate). In this time the seedlings put on vigorous growth and developed into ∼1.5 m tall saplings with plenty of leaves (see supplementary figure S2). The future climate treatment represents temperature conditions in Australia in 2050 assuming the highest 8.5 Representative Concentration Pathway (RCP) – the business as usual scenario where CO_2 reaches 940 ppm by 2100 (van Vuuren et al., 2011). The treatments maintained the diurnal variation of ambient temperature at 9 K. Further details on the growth conditions of these eucalypts are described in Aspinwall et al. (2019), prior to their study of how eucalypts respond to heatwave stress.

We will use our new experimental data to revise the LEF maps for Australia, weighting the results according to the summed area of the four species (Table 1).

2.3 Temperature response measurements

Leaf gas exchange measurements were made continuously with a LI-6400XT portable photosynthesis system (Li-Cor Inc., Lincoln, NE, USA) connected to a Walz 3010-GWK1 leaf cuvette (maximum surface area for leaf 140 cm^2; Heinz Walz GmbH, Effeltrich, Germany). The Walz cuvette was controlled via a PC using Walz software (GFS-Win v.3.47g). CO_2 concentrations were set to 400 ppmv and the flow rate through the cuvette was set to 700 μmol s^{-1}. Light was provided using Lumigrow Pro 325 LED growth lamps (LumiGrow, Novato, CA) positioned above the cuvette to provide 1000 μmol m^{-2} s^{-1} PAR as measured by the LI-6400XT cuvette's light sensor. Leaf temperature was controlled using the Walz cuvette and was programmed to increase leaf temperature in 5 K steps from 293 K to 328 K in seven minute intervals to accommodate adjustment to new steady state values of photosynthesis at each temperature. This time corresponds to the duration of intermediate length sunflecks in plant canopies (Pearcy, 1990) and also results in a common, standardised heat dose for all the leaves (Niinemets and Sun, 2015). Basal emission rates are taken as the emission rate measured at 1000 μmol m^{-2} s^{-1} PAR and 303 K.

After the gas exchange measurements, leaves were detached and their area measured using a LI-3100C leaf area meter (Li-Cor Inc.). Leaves were oven dried at 105 °C for 72 hours after which their dry weight was recorded.

Mixing ratios of isoprene by volume were determined using a high-resolution proton transfer reaction-mass spectrometer (PTR-MS, Ionicon GmbH, Innsbruck, Austria). The operating parameters of the PTR-MS were held constant during measurements, except for the secondary electron multiplier voltage, which was optimised before every calibration. The drift tube pressure, temperature and voltage were 2.2 hPa, 50 °C and 600 V. The parameter E/N was ∼125 Td (1.25×10^{-15} V cm^2) and the reaction time was ∼100 μs. The count rate of $H_3O^+ \cdot H_2O$ ions was 1–2 % of the count rate of H_3O^+ ions, which was $5.0 - 5.5 \times 10^6$ s^{-1}. Normalized sensitivities and isoprene volume mixing ratios were calculated through calibrations as described by Taipale et al. (2008) using 5 ppmv isoprene (Apel-Riemer Environmental Inc., Broomfield, CO) diluted in high

purity nitrogen (BOC Ltd, Sydney, NSW). Protonated isoprene was detected by the PTR-MS as its molecular mass plus one (i.e. M + H+1 = 69). The duty cycle for each measurement period was 5 s.

Isoprene-temperature response measurements were replicated on five or six saplings of each species in each temperature treatment group (supplementary figure S3). The Solver program (Generalized Reduced Gradient nonlinear method, default settings; Microsoft Excel for Office 365; Microsoft Corporation, Redmond, WA, USA) was used to estimate four MEGAN coefficients, C_{T1}, C_{T2}, T_{max} and C_{eo} to minimise the difference between the result of Equation 1 and the measured temperature responses, for each tree species and growth temperature treatment. The basal emission rates for each species (in μg g^{-1} h^{-1}) were normalised to the average basal emission factor for that species and its growth temperature treatment. Normalising these data scales the actual emission rates and ensures they have a common basal emission factor of unity.

2.4 Observations of isoprene mixing ratios

Few measurements of ambient isoprene exist in Australia. Hourly observations made by Proton Transfer Reaction Mass Spectrometry are available for three summertime urban field campaigns near Sydney (Figure 1). These observations will be used to evaluate model predictions using our temperature response functions of isoprene emission. Isoprene observations are available from Bringelly in the January-February of 2007, SPS1 in Westmead in the February-March of 2011 (Keywood et al., 2019), and MUMBA in Wollongong in January-February of 2013 (Paton-Walsh et al., 2017, 2018). Maximum (and average) measured temperatures were 308.9 K (295.9 K) for Bringelly, 310.0 K (295.6 K) for SPS1 and 317.2K (295.3 K) for MUMBA. Climate projections for Australia forecast increases in average temperatures with an accompanying increase in the frequency of extreme heatwave days (Bureau of Meteorology and CSIRO, 2018).

2.5 The CSIRO Chemical Transport Model (C-CTM)

The C-CTM is a modelling framework designed to predict the atmospheric concentrations of gases and aerosols due to emissions, transport, chemical production and loss, and deposition. In addition to BVOCs, the framework has successfully predicted pollen (Emmerson et al., 2019b), health effects from shipping (Broome et al., 2016) and air quality (Chambers et al., 2019). The C-CTM is driven by meteorology from the Conformal Cubic Atmospheric Model (CCAM, McGregor and Dix (2008)), taking boundary conditions from ERA-Interim. Four nested domains are used at spatial resolutions of 80 km, 27 km, 9 km and 3 km to downscale the atmospheric constituents over topography that increases with complexity at higher resolutions. The inner 3km domain contains 114 x 110 gridcells to encompass Sydney, Wollongong and the surrounding forested regions (Figure 1).

The model chemistry scheme is MOZART-T1 (Emmons et al., 2020) incorporating the latest research on isoprene oxidation pathways via additional radical production under low NO_X conditions. The aerosol framework is a two-bin sectional scheme, processing organic species by the Volatility Basis Set (Shrivastava et al., 2008) and processing inorganic species via ISORROPIA_II (Fountoukis and Nenes, 2007). The high and low NO_X aerosol mass yields for the organic species, including isoprene, are provided by Tsimpidi et al. (2010).

Australia wide anthropogenic emissions come from an inventory based on human population density on a 10 km x 10 km grid resolution (updated from Physick et al. (2002)). Anthropogenic emissions for Sydney in the 3km domain are based on the most recent NSW inventory for the year 2008 (EPA NSW, 2012). The full canopy environment version of MEGAN2.1 (Guenther et al., 2012) was built into the C-CTM to calculate the biogenic emissions (Emmerson et al., 2016). Isoprene emissions, R in a given grid cell, xy, are predicted using LEF maps in combination with the land fraction, χ occupied by 16 PFTs, j, using:

$$R = LEF_{\mathrm{x,y}} \sum_{j=1}^{nPFT} (\gamma_{\mathrm{x,y}} \times \chi_{\mathrm{j}}) \tag{5}$$

Where γ represents the sum of all activity factors for light, temperature, soil moisture, leaf area index and leaf age. The γ for soil moisture is applied using data provided by the Soil-Litter-Iso model (SLI), as recommended by Emmerson et al. (2019a). Monthly leaf area index data come from MODIS MCD15A2 version 4.

A PFT map based on the ESA CCI Land Cover distribution for the year 2010 (ESA, 2016) was created. The ESA land-cover data was used in conjunction with MODIS 44B (Vegetation Continuous Fields) product, level 5.1 for the year 2012 to provide the percentage tree, grass and shrub cover. Details on how these landcover data were aggregated or split into the 16 PFTs required by MEGAN2.1 are provided in the supplementary. Eucalypts fall under the broadleaf evergreen temperate tree category.

3 Results and discussion

3.1 Temperature response results

The fitted temperature responses for each eucalypt tree species under both current and future climate growth conditions are stronger and shifted to higher leaf temperatures than the MEGAN2.1 default response (Figure 2). The peaks in current climate γT are 40-90 $\%$ higher than default MEGAN, whilst the peaks in future climate γT are 45-200 $\%$ higher. The position of the peaks are also shifted towards higher temperature optimums, by approximately 4-9 K. For the current climate growth treatment results, running MEGAN with default settings would underestimate γT and subsequently the isoprene emission at leaf temperatures greater than 303 K. MEGAN assumes that at growth temperatures lower than the standard conditions, the amplitude of the temperature response (E_{opt}) is lowered and the peak of that response is shifted to a lower temperature (T_{opt}). These new data show for all species studied, at each growth temperature, that this is not necessarily true. Our measurements also indicate that eucalypts have evolved to cope with the high Australian temperatures and can continue to protect against heat damage via isoprene emission until $\sim$320 K. Tree species with a wide geographical coverage such as *E. camaldulensis* may also be better adapted to surviving climate change (González-Orozco et al., 2016).

Each tree in each temperature treatment group produces a similar response (numbers of trees and their temperatures at maximum γT given in Table 2). In the current climate-grown trees the temperature optimum in γT is 317 - 318 K for *E. tereticornis* and *E. smithii* decreasing at higher leaf temperatures. Both *E. camaldulensis* and *E. botryoides* persist at high γT until 328 K when measurements stopped. In the future climate-grown trees the γT peak is also $\sim$317 K and there is a

different response of *E. camaldulensis* and *E. botryoides* compared to the other species. γT in *E. camaldulensis* increases steeply with increasing leaf temperature until 321.5 K thereafter decreasing sharply. This response is common amongst the five *E. camaldulensis* in the future climate treatment, although there is scatter around this fitted response. The *E. camaldulensis* result will dominate the weighted variables used in the modelling because of its larger geographic distribution (Table 1). We discuss the impact of this sharp downturn in γT at high temperatures in section 3.3.

3.2 Isoprene emission rates

The basal isoprene emission rates (BER) in μg g^{-1} h^{-1} were measured at the standard 303 K and 1000 μmol m^{-2} s^{-1} PAR (Table 2). As the current climate growth treatment represents current day climatic conditions, we only compare these with measurements made previously on the same species. The *E. tereticornis* BER measurements are lower than those made by Nelson et al. (2000) and Jiang (2020); however our *E. camaldulensis* BER measurements are around 10 μg g^{-1} h^{-1} higher than that listed by Benjamin et al. (1996), and our *E. botryoides* BER measurements are $\sim$37 μg g^{-1} h^{-1} higher than that measured by He et al. (2000). He et al. (2000) used a mixture of young and mature leaves in their experiments, which could be one explanation for the difference in emission rates as young leaves are expected to be higher emitters than older leaves in *Eucalyptus* (Street et al., 1997). However, as the growth conditions (particularly light and temperature) and measurement protocols between this study and He et al. (2000) were different (we directly measured BER with a leaf cuvette at 303 K and 1000 μmol m^{-2} s^{-1} PAR while He et al. (2000) used a dynamic chamber and scaled emissions to 303 K and 1000 μmol m^{-2} s^{-1} PAR using algorithms from Guenther et al. (1993)), it is difficult to undertake a direct comparison. However, our measurements put the four eucalypt species into the high emission category.

To create new isoprene emission factor maps suitable for the modelling, we convert the BERs into landscape emission factors (LEF$_{\text{isop}}$). The average BER for each growth treatment is weighted according to their geographical areas in Table 1. BERs are then converted into LEFs using the leaf mass per unit area (LMA) in g m^{-2} and scaled with LAI in m^2 m^{-2}, similar to Emmerson et al. (2018). The isoprene emission factor for trees in each temperature treatment is given by tree_EF$_{\text{isop}}$:

$$tree\_EF_{\text{isop}} = BER \times LAI \times LMA \tag{6}$$

In the C-CTM, northern Australian vegetation is represented by broadleaf shrubs (30 – 40 %) and C4 grasses (50 to 80 % in some locations). If the isoprene emission factor maps are only based on the new eucalypt BERs, these are unlikely to be representative of shrubs and grasses. Here we ensure the non-tree fraction of grid cells in Australia are not impacted by these changes using the tree fraction (treefrac) from the ESA product.

$$LEF_{\text{isop}} = (tree\_EF_{\text{isop}} \times treefrac) + (orig\_EF_{\text{isop}} \times (1 - treefrac)) \tag{7}$$

This leaves the fraction of original isoprene LEFs (orig_EF$_{\text{isop}}$) untouched for grass and shrub PFTs.

3.3 Impacts of changing C_{T1}, C_{T2}, T_{max} and C_{eo}

Table 3 shows the results of fitting C_{T1}, C_{T2}, T_{max} and C_{eo} compared to the default MEGAN values. These new fitted data are for the four tree species in the experiment, weighted according to their coverage in Table 1.The new average LEFs from our four eucalypt species are 31 - 48 % lower than the default average MEGAN LEF we use in the base run for the 3km Sydney domain. Previous modelling showed that a 40 % reduction in isoprene was needed to better match the observations from our three field campaigns Emmerson et al. (2019a).

The value fitted for C_{T2} is very high (1158.36 kJ mol^{-1}) in the future climate treatment compared with the current climate treatment (167.11 kJ mol^{-1}) and default MEGAN (230 kJ mol^{-1}), due to the *E. camaldulensis* measurements in Figure 2. To assess whether C_{T2} should be re-fitted we examine the impacts of changing each of these variables one at a time using a MEGAN boxmodel designed in Jiang (2020). As the impacts of the new measurements are strongest at higher temperatures, we assume conditions from the hottest day in the MUMBA campaign (January 18th). The MEGAN boxmodel runs for 24 hours, and the results given as percentage changes to the maximum isoprene emission in Table 3. For the given fitted values on this day, the C_{T1} variable has the least and C_{eo} has the most impact on isoprene emissions. The high C_{T2} value in the future climate treatment will not be refitted, as the incurred 19 % decrease in isoprene is small compared with the 282 % increase caused by C_{eo}. Individually C_{eo} has the greatest impact on isoprene emissions but is regulated by increasing T_{max} when used in tandem with other variables. However, when all variables operate together the overall impact is an $\sim$80 % increase in isoprene emissions for both current and future climate growth conditions. Inclusion of the average LEF reduces the maximum isoprene emission by 7 % in the current climate treatment conditions and increases by 23 % in the future climate treatment conditions on the default.

3.4 Model experiment set-up

Seven model experiments are defined (Table 4) and are run for the periods of the field campaigns described in section 2.4. We model the impacts of using the new current and future climate treatment temperature response variables separately from the impacts of the new LEFs on atmospheric isoprene mixing ratios. For experiments 1 to 5, we use the same hourly meteorology, current day tree distribution maps and LAI datasets to drive the C-CTM. This allows us to separate the temperature effect in isoprene emissions from other influences which may change in a future climate. The intention is to investigate changes in isoprene emissions resulting from the temperature response results, not to combine these with future land-use changes and how the hourly meteorology will be impacted by climate change. However, in experiment 6 we use a simple delta-scaling approach to address how a future climate may impact the driving input temperatures to MEGAN.

We take the average change (δ2050) in projected summertime surface temperatures for Australia under the RCP 8.5 scenario from eight models in the Coupled Model Intercomparison Project 5 (CMIP5) (for details see supplementary). Delta-scaling adds $\sim$2 K to the surface temperatures near Sydney. We only scale the surface temperature, thus experiment 6 is not a 2050 representation of the whole atmosphere. This restricts the use of the delta-scaled temperatures as a MEGAN input and not the temperature used for chemical reactions, as mass balance difficulties would occur by not also delta-scaling the pressure and air

density through the height of the atmosphere. We estimate the reaction rate of isoprene with OH (calculated as 2.54×10^{-11} exp(410/T) in MOZART-T1) would decrease by 1.7 % with the 3.5 K temperature rise between our current and future climate growth treatments.

The climate2050 run does not include the associated increases in CO_2 mixing ratios, to be consistent with our measurements that were also not conducted in a higher CO_2 atmosphere. A 7th simulation assumes a 550 ppm CO_2 atmosphere on top of the delta-scaled surface temperatures, employing the Heald et al. (2009) method for calculating short and long term CO_2 activity factors, γC. Fixing the atmospheric CO_2 to 550 ppm reduces the isoprene emissions by 5 % in the short term and 13 % in the long term.

If the leaf temperature is varied within Equations 1-4 and γT is multiplied by the LEF, the impacts of experiments 1-5 on isoprene emission start at about 283 K (Figure 3). Experiment 6 follows the FC_γT+LEF profile. Here, the new current and future climate LEFs are normalised by the default MEGAN LEF. The default MEGAN profile has a peak isoprene emission at 311 K. The CC_γT and FC_γT experiments cause the isoprene emission peak to shift to 324 K, with three times the default emission value. The sharp downturn in isoprene emission in the FC_γT and FC_γT+LEF experiments after 324 K are due to the high γT of *E. camaldulensis* depicted in Figure 2. However, these results will not impact the C-CTM runs as no hourly temperature in our three field campaigns exceeds 317 K. Most of the impacts on the C-CTM runs will occur in the 288 - 308 K range. Whilst there is a very small decrease in the CC_γT response compared with the default MEGAN profile at temperatures less than 300 K, overall we expect more isoprene to be emitted in the CC_γT and FC_γT experiments over the default MEGAN profile. While it is intuitive to expect less isoprene will be emitted in the CC_γT+LEF and FC_γT+LEF experiments over the base run (from Figure 3), this may not be the case due to spatial heterogeneity in the new current and future climate LEF maps. The LEFs used in Figure 3 are based on the domain spatial average value, however the LEFs in experiments 3 and 5 are based on the distribution of LAI from equation 6, whilst experiments 1, 2 and 4 use the original MEGAN LEF distribution. The results from experiments 3 and 5 certainly certainly show a sustained isoprene decrease below 314 K and 311 K respectively. Distance from source to receptor, transport and dilution will all impact results, and are determined by running the C-CTM.

3.5 C-CTM results

The C-CTM is compiled with changes to MEGAN implemented according to Table 3, run for experiments 1-6 (Table 4) and the isoprene time series is extracted at each field campaign site. The modelled mean diurnal profiles of isoprene are then compared to the mean diurnal observations taken at each field campaign (Figure 4). Instrument calibrations/blanks are taken at least twice a day, incurring frequent regular gaps in observed isoprene. The CC_γT variables only increase the isoprene mixing ratios when temperatures exceed 303 K (from Figure 3). This has changed the shape of the diurnal profiles of each field campaign in different ways, but generally the CC_γT and CC_γT+LEF experiments have increased the diurnal modelled to observed r^2 when compared with the r^2 between the base run and observations. The average modelled isoprene in the CC_γT+LEF run is within $\pm$ 1 standard deviation of the observations 90 – 100 % of the time during Bringelly and SPS1, and 33 % during MUMBA which continues to exhibit high bias (supplementary figure S4). In MUMBA, the CC_γT increases the isoprene mixing ratios above the base run between 11:00 and 17:00 AEDT in the heat of the day. Very hot temperatures

during the day can often be accompanied by strong gusty winds from the Australian interior. The hottest campaign day, 18th January 2013 during MUMBA was associated with the highest average hourly wind measurement of 8 m s^{-1}. Hot and windy conditions would cause lots of sun-flecking within the tree canopy, causing sudden temperature spikes on the leaf surface. Physiologically, the increased production of isoprene during temperature and light spikes helps to maintain photosynthesis (Behnke et al., 2010) during times of mild stresses (Loreto and Fineschi, 2015), above and beyond leaf cooling via transpiration processes (Sharkey et al., 2008). High isoprene emitters can better survive prolonged heatwaves (Yáñez-Serrano et al., 2019), although the Aspinwall et al. (2019) study on our four eucalypt species showed trees grown under future climate conditions suffered greater heatwave damage than the same species in current climate conditions.

During all campaigns the CC_γT results have decreased the isoprene from the base runs in the morning between 08:00 and 11:00 AEDT, because these temperatures are less than 303 K where the γT are less than the default MEGAN profile (Figure 3). The CC_γT+LEF experiments represent current day conditions, with roughly the correct magnitude (MUMBA excepted) of predicted isoprene and best statistical fit compared with the observations. The FC_γT+LEF experiment has produced more daytime isoprene than the base run contrary to the prediction in Figure 3, because the distribution of isoprene LEFs near the field campaign sites is different to the default MEGAN LEFs. The climate2050 experiment adds between 110 - 170 % more isoprene during the day, or approximately 2 ppb. The addition of a higher CO_2 atmosphere has reduced the daytime isoprene by 15 - 26 % from the climate2050 run, across the three campaigns.

The MUMBA and SPS1 base diurnal profiles show too much isoprene in the model overnight compared to observed mean values, particularly in the period midnight to 06:00 AEDT. This is because there is more isoprene in the model atmosphere than was quenched by the OH radical before the OH production ceased at sundown. The isoprene becomes more concentrated at the surface because of the reduced boundary layer height; the apparent increase between midnight and 03:00 AEDT is not due to night-time isoprene emissions. Conversely a slight rise in the model boundary layer at 04:00 AEDT in SPS1 causes dilution of the atmospheric isoprene. While there are few measurements of isoprene during these pre-dawn periods, it is unlikely isoprene is present. Only when daytime isoprene is reduced in the CC_γT+LEF experiment do we see the apparent night-time isoprene is decreased.

We investigate the spatial changes to isoprene, O_3 and biogenic SOA in an implied future by subtracting results from the CC_γT+LEF experiment from the climate2050 experiment during the period of the SPS1 campaign (Figure 5). These emissions, mixing ratios and aerosol concentrations represent campaign averages from SPS1. We also show the smaller differences found between the FC_γT+LEF and CC_γT+LEF runs. The climate2050 experiment causes up to 5.2 mg m^{-2} h^{-1} in isoprene emissions to the immediate north of Sydney (Figure 5d), but there are also increases in the north of Australia (Figure 5c). The largest changes of 15.8 ppb in isoprene occur in sparsely inhabited northern Australia (Figure 5g), and in urbanised pockets to the south and east, where Sydney is located. The urbanisation becomes important when the increased isoprene reacts with NO_X in the atmosphere causing a peak 9 ppb increase to O_3 near Sydney with the climate2050 differences (Figure 5l). However, the FC_γT+LEF differences (Figure 5i) show a 0.5 ppb decrease in O_3 in northern Australia via quenching by the additional isoprene. Few inhabitants reside in northern Australia, meaning O_3 production via anthropogenic NO_X is minimised. Soil NO_X emissions are low in northern Australia as agricultural practices largely occur in the south east and south west of Australia.

The O_3 deficit is still visible in the very north east of Australia in the climate2050 difference run (Figure 5k). The increase in biogenic SOA occurs mainly in the north of Australia where up to 0.21 μg m^{-3} more aerosol is predicted by the climate2050 experiment than the CC_γT+LEF experiment (Figure 5o).

The size fraction of most secondary organic aerosol fits within the $PM_{2.5}$ classification, defined as particulate matter with an aerodynamic diameter less than 2.5 μm. Australia sets National Environmental Protection Measures (NEPMs) for $PM_{2.5}$ and O_3 to ensure a healthy standard of air quality for the population. The NEPM for O_3 is 100 ppb as a 1-hour average, and 25 μg m^{-3} as a 24-hour average for $PM_{2.5}$, with a goal of reducing the $PM_{2.5}$ limit to 20 μg m^{-3} by 2025. We examine the increases brought about by climate induced isoprene in the two cities impacted by most of these changes, Sydney and Darwin, in Australia's north (Figure 6).

The air quality index (AQI = NEPM/pollutant concentration x 100) in Sydney and Darwin is classed as 'very good' (AQI <33) for both pollutants (years 2009 – 2014), with an improving trend for O_3 but a declining trend for $PM_{2.5}$ (Keywood et al., 2016). Darwin is a small city, and the biogenic component of O_3 changes are less than 2 ppb. However peak O_3 in Sydney increases by 10 – 15 ppb as an hourly average in the FC_γT+LEF differences, but by 12 - 17 ppb in the climate2050_γC differences and by as much as 15 - 21 ppb in the climate2050 differences (Figure 6a,b). These increases represent 10 - 21 % of the O_3 NEPM, and show that by doing nothing (e.g. tree type and coverage or air quality policies do not change) and allowing the temperatures to rise, large cities will likely encounter more NEPM exceedances. The solution is not to remove native trees as they provide social amenity and have cultural significance for indigenous populations. Rather, their emissions must be accommodated via atmospheric NO_X reductions. New urban developments should consider the BVOC emission potential of trees before planting (Paton-Walsh et al., 2019), taking into account that non or low emitting trees may not withstand climate induced heatwaves (Peñuelas and Munné-Bosch, 2005).

The SOA from isoprene is a small fraction of the $PM_{2.5}$ limit (shown here as 24-hour averages), though of the BVOC aerosol yields, isoprene is not expected to dominate. The aerosol yields from monoterpenes are 10-20 times higher than the isoprene yield and the monoterpene emission would increase in a warming climate (not investigated here). The climate2050 differences (and climate2050_γC) show days with an increase of 0.42 μg m^{-3} in Sydney and 0.14 μg m^{-3} in Darwin (2 % and 1 % of the $PM_{2.5}$ 2025 NEPM, respectively).

4 Conclusions

We have measured the isoprene emission response to controlled increases in temperature from four eucalypt species, two of which have a large geographical growing extent in Australia. The trees were grown in temperatures representing the current climate summertime conditions in Australia and in temperatures representing the projected summertime conditions of +3.5 K warming under the business as usual RCP 8.5 scenario. Climate projections for Australia forecast increases in average temperatures with an accompanying increase in the frequency of extreme heatwave days (Bureau of Meteorology and CSIRO, 2018). This will likely increase in the number of days above 303 K.

The current condition experiments demonstrated a change in the isoprene emission response to temperature as compared with the default parameterisation in MEGAN. This is not a surprise, as MEGAN is built to represent a range in ecosystem responses, but may go some way to explain why difficulties have been encountered when modelling isoprene in Australia previously. Both the current and future climate growth treatment temperature responses shifted the peak in γT by 4-9 K, signifying that these four eucalypt species were observed to continue emitting isoprene until well past the default maximum temperature for emission at 313 K. This suggests the eucalypts used in this study have evolved to protect against higher temperatures as expected with climate change.

Higher basal emission rates were measured in three of the eucalypt species in our experiment than have been previously measured. However, the conversion of these average weighted emission rates to LEFs for use in the C-CTM, resulted in a lower average LEF than are currently being used in the base run. This is due to low biomass measured on our leaves, and because the isoprene emission factors from regions described as shrubs or grasslands were not altered. The spatial distribution of the new LEFs were based on the LAI distribution, different to the default MEGAN isoprene LEF map.

The model results using the new current climate growth temperature responses improved the statistical fits of the diurnal profiles compared to the measurements in average isoprene across our three field campaign periods. The overall magnitude of the modelled profile was also brought into better agreement with observations in combination with the new current climate growth LEFs. MEGANv2.1 essentially works using a series of variables dependant on vegetation type and biogenic compound emission traits, and the results here suggest that the four MEGAN variables altered in our experiments could also become ecosystem or location specific.

Our measurements were conducted on sapling trees which may exhibit higher isoprene emissions than adult trees when emission rates are expressed on leaf mass basis but not on a leaf area basis (Street et al., 1997). Street et al. (1997) explained this through younger leaves having a higher specific leaf area than older leaves because eucalypts exhibit heterophylly (the foliage leaves on the same plant are of two distinctly different types). The apparent difference in emission rates between young and old leaves could be a consequence of morphology rather than biochemistry, so we expect the trend between the current and future climate growth emissions to be similar amongst trees of all ages. Our model experiments simulating isoprene emissions in a 2050 climate examined the differences between these runs and the CC_γT+LEF experiment. Three future experiments were conducted, the first using current day meteorology, the second using a delta-scaled surface temperature change to projected 2050 summertime temperatures, and the third using a 550 ppm atmospheric CO_2 on top of the delta scaled temperatures. The FC_γT+LEF experiment showed increases in isoprene emissions in the north of Australia, as well as closer to Sydney. These increases led to O_3 rising 10 – 15 ppb close to Sydney as a result of the increased isoprene, whilst decreasing in sparsely populated northern Australia through quenching by the additional isoprene. The climate2050 experiment showed much larger increases in isoprene, O_3 and biogenic SOA across Australia, tempered slightly by the addition of increased atmospheric CO_2. Delta-scaling the surface temperatures was the simplest way of conducting future climate experiments. Future work should investigate getting a downscaled version of the 2050 atmosphere from CCAM which would provide the hourly meteorology throughout the atmosphere that the C-CTM requires.

The future is expected to bring increased temperatures, CO_2 and land use changes. Sharkey and Monson (2014) evaluated the isoprene trade-off in each of these scenarios and concluded the temperature effects would dominate. O_3 is a secondary product of isoprene oxidation, and is currently maintained at healthy levels in Australia. In order to maintain these levels, air quality policy should investigate methods to reduce anthropogenic NO_X emissions in city regions to accommodate these climate change induced increases in BVOC emissions. In addition, tree planting efforts in new urban developments should also consider the BVOC emission potential of prospective trees.

Code availability. TEXT

Data availability. The LAI data product was retrieved from MCD15A2 version 4 from the online Data Pool, courtesy of the NASA Land Processes Distributed Active Archive Center (LP DAAC), USGS/Earth Resources Observation and Science (EROS) Center, Sioux Falls, South Dakota, https://lpdaac.usgs.gov/data_access/data_pool

Code and data availability. TEXT

Sample availability. TEXT

Author contributions. KME and MP devised the modelling study and wrote the manuscript. KME conducted the modelling. MP, MJA, SP and MGT conducted the experimental work. MJA, SP and MGT edited the manuscript.

Competing interests. The authors have no competing interests.

Disclaimer. TEXT

Acknowledgements. KME thanks Christine Wiedinmyer at the University of Colorado, Boulder for assistance with the ESA landcover product data and John Clarke at CSIRO for helpful discussions on using the climate projections data.

References

Arneth, A., Schurgers, G., Lathiere, J., Duhl, T., Beerling, D. J., Hewitt, C. N., Martin, M., and Guenther, A.: Global terrestrial isoprene emission models: sensitivity to variability in climate and vegetation, Atmospheric Chemistry and Physics, 11, 8037–8052, https://doi.org/10.5194/acp-11-8037-2011, https://www.atmos-chem-phys.net/11/8037/2011/, 2011.

Aspinwall, M. J., Pfautsch, S., Tjoelker, M. G., Vårhammar, A., Possell, M., Drake, J. E., Reich, P. B., Tissue, D. T., Atkin, O. K., Rymer, P. D., Dennison, S., and Van Sluyter, S. C.: Range size and growth temperature influence Eucalyptus species responses to an experimental heatwave, Global Change Biology, 25, 1665–1684, https://doi.org/10.1111/gcb.14590, https://onlinelibrary.wiley.com/doi/abs/10.1111/gcb.14590, 2019.

Atlas of Living Australia: Eucalyptus camaldulensis, https://bie.ala.org.au/species/http://id.biodiversity.org.au/node/apni/2921040 (Accessed 6 September 2019), 2019.

Bauwens, M., Stavrakou, T., Müller, J.-F., Van Schaeybroeck, B., De Cruz, L., De Troch, R., Giot, O., Hamdi, R., Termonia, P., Laffineur, Q., Amelynck, C., Schoon, N., Heinesch, B., Holst, T., Arneth, A., Ceulemans, R., Sanchez-Lorenzo, A., and Guenther, A.: Recent past (1979–2014) and future (2070–2099) isoprene fluxes over Europe simulated with the MEGAN–MOHYCAN model, Biogeosciences, 15, 3673–3690, https://doi.org/10.5194/bg-15-3673-2018, https://www.biogeosciences.net/15/3673/2018/, 2018.

Behnke, K., Loivamäki, M., Zimmer, I., Rennenberg, H., Schnitzler, J.-P., and Louis, S.: Isoprene emission protects photosynthesis in sunfleck exposed Grey poplar, Photosynthesis research, 104, 5—17, https://doi.org/10.1007/s11120-010-9528-x, https://doi.org/10.1007/s11120-010-9528-x, 2010.

Benjamin, M. T., Sudol, M., Bloch, L., and Winer, A. M.: Low-emitting urban forests: A taxonomic methodology for assigning isoprene and monoterpene emission rates, Atmospheric Environment, 30, 1437—-1452, https://doi.org/10.1016/1352-2310(95)00439-4, 1996.

Broome, R. A., Cope, M. E., Goldsworthy, B., Goldsworthy, L., Emmerson, K., Jegasothy, E., and Morgan, G. G.: The mortality effect of ship-related fine particulate matter in the Sydney greater metropolitan region of NSW, Australia, Environ Int, 87, 85–93, 2016.

Brophy, J. J., House, A. P. N., Boland, D. J., and Lassak, E. V.: Digest of the essential oils of 111 species from northern and eastern Australia., in Eucalyptus Leaf Oils: Use, Chemistry, Distillation and Marketing, D.J. Boland, et al. (Eds.), pp. 129–155, Inkarta Press, Melbourne, 1991.

Bureau of Meteorology and CSIRO: State of the Climate 2018, http://www.bom.gov.au/state-of-the-climate/index.shtml (Accessed 18 October 2019), 2018.

Chambers, S. D., Guerette, E.-A., Monk, K., Griffiths, A. D., Zhang, Y., Duc, H., Cope, M., Emmerson, K. M., Chang, L. T., Silver, J. D., Utembe, S., Crawford, J., Williams, A. G., and Keywood, M.: Skill-Testing Chemical Transport Models across Contrasting Atmospheric Mixing States Using Radon-222, Atmosphere, 10, http://www.mdpi.com/2073-4433/10/1/25, 2019.

Department of Agriculture and Water Resources: Australia's State of the Forests Report 2018., https://www.agriculture.gov.au/abares/forestsaustralia/sofr/sofr-2018, accessed 2/12/2019., 2018.

Emmerson, K. M., Galbally, I. E., Guenther, A. B., Paton-Walsh, C., Guérette, E.-A., Cope, M. E., Keywood, M. D., Lawson, S. J., Molloy, S. B., Dunne, E., Thatcher, M., Karl, T., and Maleknia, S. D.: Current estimates of biogenic emissions from eucalypts uncertain for southeast Australia, Atmos. Chem. Phys., 16, 6997–7011, https://doi.org/10.5194/acp-16-6997-2016, 2016.

Emmerson, K. M., Cope, M. E., Galbally, I. E., Lee, S., and Nelson, P. F.: Isoprene and monoterpene emissions in south-east Australia: comparison of a multi-layer canopy model with MEGAN and with atmospheric observations, Atmos. Chem. Phys., 18, 7539–7556, https://doi.org/10.5194/acp-18-7539-2018, 2018.

Emmerson, K. M., Palmer, P. I., Thatcher, M., Haverd, V., and Guenther, A. B.: Sensitivity of isoprene emissions to drought over south-eastern Australia: Integrating models and satellite observations of soil moisture, Atmos Environ, 209, 112–124, https://doi.org/10.1016/j.atmosenv.2019.04.038, 2019a.

Emmerson, K. M., Silver, J. D., Newbigin, E., Lampugnani, E. R., Suphioglu, C., Wain, A., and Ebert, E.: Development and evaluation of pollen source methodologies for the Victorian Grass Pollen Emissions Module VGPEM1.0, Geoscientific Model Development, 12, 2195–2214, https://doi.org/10.5194/gmd-12-2195-2019, https://www.geosci-model-dev.net/12/2195/2019/, 2019b.

Emmons, L. K., Orlando, J. J., Tyndall, G., Schwantes, R. H., Lamarque, J.-F., Marsh, D., Mills, M. J., Tilmes, S., Buchholz, R. R., Gettelman, A., Garcia, R., Simpson, I., Meinardi, S., and Pétron, G.: The Chemistry Mechanism in the Community Earth System Model version 2, Submitted to J. Advances in Modeling Earth Systems, CESM2 special issue, 2020.

EPA NSW: air-emissions-inventory, NSW Environment Protection Authority, https://www.epa.nsw.gov.au/your-environment/air/air-emissions-inventory (Accessed 4 September 2019), 2012.

ESA: CI Land Cover dataset (v 1.6.1), https://www.esa-landcover-cci.org/?q=node/169 (Accessed 4 September 2019), 2016.

Evans, R. C., Tingey, D. T., Gumpertz, M. L., and Burns, W. F.: Estimates of Isoprene and Monoterpene Emission Rates in Plants, Botanical Gazette, 143, 304–310, https://doi.org/10.1086/botanicalgazette.143.3.2474826, https://doi.org/10.1086/botanicalgazette.143.3.2474826, 1982.

Fountoukis, C. and Nenes, A.: ISORROPIA II: a computationally efficient thermodynamic equilibrium model for K^+-;Ca^{2+}-;Mg^{2+}-;NH_4^+-;Na^+-;SO_4^{2-}-;NO_3^--;Cl^--;H_2O aerosols, Atmospheric Chemistry and Physics, 7, 4639–4659, https://doi.org/10.5194/acp-7-4639-2007, https://www.atmos-chem-phys.net/7/4639/2007/, 2007.

González-Orozco, C. E., Pollock, L. J., Thornhill, A. H., Mishler, B. D., Knerr, N., Laffan, S. W., Miller, J. T., Rosauer, D. F., Faith, D. P., Nipperess, D. A., Kujala, H., Linke, S., Butt, N., Külheim, C., Crisp, M. D., and Gruber, B.: Phylogenetic approaches reveal biodiversity threats under climate change, Nature Climate Change, 6, 1110–1114, https://doi.org/10.1038/nclimate3126, 2016.

Guenther, A. B., Zimmerman, P. R., Harley, P. C., Monson, R. K., and Fall, R.: Isoprene and monoterpene emission rate variability: Model evaluations and sensitivity analyses, Journal of Geophysical Research: Atmospheres, 98, 12 609–12 617, https://doi.org/10.1029/93JD00527, https://agupubs.onlinelibrary.wiley.com/doi/abs/10.1029/93JD00527, 1993.

Guenther, A. B., Jiang, X., Heald, C. L., Sakulyanontvittaya, T., Duhl, T., Emmons, L. K., and Wang, X.: The Model of Emissions of Gases and Aerosols from Nature version 2.1 (MEGAN2.1): an extended and updated framework for modeling biogenic emissions, Geoscientific Model Development, 5, 1471–1492, https://doi.org/10.5194/gmd-5-1471-2012, https://www.geosci-model-dev.net/5/1471/2012/, 2012.

He, C., Murray, F., and Lyons, T.: Monoterpene and isoprene emissions from 15 Eucalyptus species in Australia, Atmospheric Environment, 34, 645 – 655, https://doi.org/https://doi.org/10.1016/S1352-2310(99)00219-8, http://www.sciencedirect.com/science/article/pii/S1352231099002198, 2000.

Heald, C. L., Wilkinson, M. J., Monson, R. K., Alo, C. A., Wang, G., and Guenther, A.: Response of isoprene emission to ambient CO2 changes and implications for global budgets, Global Change Biology, 15, 1127–1140, https://doi.org/10.1111/j.1365-2486.2008.01802.x, https://onlinelibrary.wiley.com/doi/abs/10.1111/j.1365-2486.2008.01802.x, 2009.

Jiang, M. Belinda Medlyn, John Drake, Remko Duursma, Ian Anderson, Craig Barton, Matthias Boer, Yolima Carrillo, L Castañeda-Gómez, L Collins, Kristine Crous, Martin de Kauwe, Bruna dos Santos, Kathryn Emmerson, S.L Facey, A.N Gherlenda, Teresa Gimeno, S Hasegawa, S Johnson, A Kannaste, Catriona A Macdonald, K Mahmud, Ben Moore, Loic Nazaries, Elizabeth Neilson, Uffe N. Nielsen, Ülo Niinemets, N.J Noh, R Ochoa-Hueso, V.S Pathare, Elise Pendall, J Pihlblad, J Pineiro, Jeff Powell, Sally Power, Peter Reich, A.A Renchon, Markus Riegler, Riikka Rinnan, Paul Rymer, R.L Salomón, Brajesh Singh, Benjamin Smith, Mark Tjoelker, J.K.M Walker, A

Wujeska-Klaus, J Yang, Soenke Zaehle, and David Ellsworth: The fate of carbon in a mature forest under carbon dioxide enrichment, accepted in Nature, 2020.

Karkik, J. and Winer, A.: Measured isoprene emission rates of plants in California landscapes: comparison to estimates from taxonomic relationships, Atmospheric Environment, 35, 1123 – 1131, https://doi.org/https://doi.org/10.1016/S1352-2310(00)00258-2, 2001.

Kesselmeier, J. and Staudt, M.: Biogenic Volatile Organic Compounds (VOC): An Overview on Emission, Physiology and Ecology, Journal of Atmospheric Chemistry, 33, 23–88, https://doi.org/10.1023/A:1006127516791, 1999.

Keywood, M., Selleck, P., Reisen, F., Cohen, D., Chambers, S., Cheng, M., Cope, M., Crumeyrolle, S., Dunne, E., Emmerson, K., Fedele, R., Galbally, I., Gillett, R., Griffiths, A., Guerette, E.-A., Harnwell, J., Humphries, R., Lawson, S., Miljevic, B., Molloy, S., Powell, J., Simmons, J., Ristovski, Z., and Ward, J.: Comprehensive aerosol and gas data set from the Sydney Particle Study, Earth System Science Data, 11, 1883–1903, https://doi.org/10.5194/essd-11-1883-2019, https://www.earth-syst-sci-data.net/11/1883/2019/, 2019.

Keywood, M. D., Hibberd, M. H., and Emmerson, K. M.: Australia: State of the environment 2016 – Atmosphere, independent report to the Australian Government Minister for the Environment and Energy, Australian Government Department of the Environment and Energy, Canberra, https://doi.org/doi:10.4226/94/58b65c70bc372, 2016.

Loreto, F. and Fineschi, S.: Reconciling functions and evolution of isoprene emission in higher plants, New Phytologist, 206, 578–582, https://doi.org/10.1111/nph.13242, https://nph.onlinelibrary.wiley.com/doi/abs/10.1111/nph.13242, 2015.

McGregor, J. L. and Dix, M. R.: An updated description of the Conformal-Cubic Atmospheric Model in High Resolution Simulation of the Atmosphere and Ocean, Hamilton K and Ohfuchi W (Eds), pp. 51–76,, Springer, 2008.

Millet, D. B., Baasandorj, M., Hu, L., Mitroo, D., Turner, J., and Williams, B. J.: Nighttime Chemistry and Morning Isoprene Can Drive Urban Ozone Downwind of a Major Deciduous Forest, Environmental Science & Technology, 50, 4335–4342, https://doi.org/10.1021/acs.est.5b06367, https://doi.org/10.1021/acs.est.5b06367, pMID: 27010702, 2016.

Nelson, P. F., Nancarrow, P. C., Haliburton, B., Tibbet, A. R., Chase, D., and Trieu, T.: Biogenic emissions from trees and grasses. CSIRO investigation Report ET/IR297, Tech. rep., 2000.

Niinemets, Ü. and Sun, Z.: How light, temperature, and measurement and growth [CO2] interactively control isoprene emission in hybrid aspen, Journal of experimental botany, 66, 841–51, https://doi.org/10.1093/jxb/eru443, 2015.

Niinemets, U., Arneth, A., Kuhn, U., Monson, R. K., Peñuelas, J., and Staudt, M.: The emission factor of volatile isoprenoids: stress, acclimation, and developmental responses, Biogeosciences, 7, 2203–2223, https://doi.org/10.5194/bg-7-2203-2010, https://www.biogeosciences.net/7/2203/2010/, 2010.

Paton-Walsh, C., Guérette, E.-A., Kubistin, D., Humphries, R., Wilson, S. R., Dominick, D., Galbally, I., Buchholz, R., Bhujel, M., Chambers, S., Cheng, M., Cope, M., Davy, P., Emmerson, K., Griffith, D. W. T., Griffiths, A., Keywood, M., Lawson, S., Molloy, S., Rea, G., Selleck, P., Shi, X., Simmons, J., and Velazco, V.: The MUMBA campaign: measurements of urban, marine and biogenic air, Earth System Science Data, 9, 349–362, https://doi.org/10.5194/essd-9-349-2017, https://www.earth-syst-sci-data.net/9/349/2017/, 2017.

Paton-Walsh, C., Guérette, E.-A., Emmerson, K., Cope, M., Kubistin, D., Humphries, R., Wilson, S., Buchholz, R., Jones, N. B., Griffith, D. W. T., Dominick, D., Galbally, I., Keywood, M., Lawson, S., Harnwell, J., Ward, J., Griffiths, A., and Chambers, S.: Urban Air Quality in a Coastal City: Wollongong during the MUMBA Campaign, Atmosphere, 9, http://www.mdpi.com/2073-4433/9/12/500, 2018.

Paton-Walsh, C., Rayner, P., Simmons, J., Fiddes, S., Schofield, R., Bridgman, H., Beaupark, S., Broome, R., Chambers, S., Chang, L.-C., Cope, M., Cowie, C., Desservettaz, M., Dominick, D., Emmerson, K., Forehead, H., Galbally, I., Griffiths, A., Guérette, E.-A., Haynes, A., Heyworth, J., Jalaludin, B., Kan, R., Keywood, M., Monk, K., Morgan, G., Nguyen Duc, H., Phillips, F., Popek, R., Scorgie, Y., Silver,

J., Utembe, S., Wadlow, I., Wilson, S., and Zhang, Y.: A Clean Air Plan for Sydney: An Overview of the Special Issue on Air Quality in New South Wales, Atmosphere, 10, https://doi.org/10.3390/atmos10120774, 2019.

Pearcy, R. W.: Sunflecks and Photosynthesis in Plant Canopies, Annual Review of Plant Physiology and Plant Molecular Biology, 41, 421–453, https://doi.org/10.1146/annurev.pp.41.060190.002225, https://doi.org/10.1146/annurev.pp.41.060190.002225, 1990.

Peñuelas, J. and Munné-Bosch, S.: Isoprenoids: an evolutionary pool for photoprotection, Trends in Plant Science, 10, 166 – 169, https://doi.org/https://doi.org/10.1016/j.tplants.2005.02.005, 2005.

Physick, B., Edwards, M., and Cope, M.: A Screening Procedure for Monitoring Ozone and Nitrogen Dioxide in "Small-to Medium-sized" Cities: Phase II application of the procedure, CSIRO, Australia., Tech. rep., CSIRO Marine and Atmospheric Research, 2002.

Sharkey, T. D. and Monson, R. K.: The future of isoprene emission from leaves, canopies and landscapes, Plant, Cell & Environment, 37, 1727–1740, https://doi.org/10.1111/pce.12289, https://onlinelibrary.wiley.com/doi/abs/10.1111/pce.12289, 2014.

Sharkey, T. D. and Monson, R. K.: Isoprene research – 60 years later, the biology is still enigmatic, Plant, Cell & Environment, 40, 1671–1678, https://doi.org/10.1111/pce.12930, https://onlinelibrary.wiley.com/doi/abs/10.1111/pce.12930, 2017.

Sharkey, T. D., Wiberley, A. E., and Donohue, A. R.: Isoprene Emission from Plants: Why and How, Ann Bot, 101, 5–18, https://doi.org/10.1093/aob/mcm240, 2008.

Shrivastava, M. K., Lane, T. E., Donahue, N. M., Pandis, S. N., and Robinson, A. L.: Effects of gas particle partitioning and aging of primary emissions on urban and regional organic aerosol concentrations, Journal of Geophysical Research: Atmospheres, 113, https://doi.org/10.1029/2007JD009735, https://agupubs.onlinelibrary.wiley.com/doi/abs/10.1029/2007JD009735, 2008.

Street, R. A., Hewitt, C. N., and Mennicken, S.: Isoprene and monoterpene emissions from a eucalyptus plantation in Portugal, Journal of Geophysical Research: Atmospheres, 102, 15 875–15 887, https://doi.org/10.1029/97JD00010, https://agupubs.onlinelibrary.wiley.com/doi/abs/10.1029/97JD00010, 1997.

Taipale, R., Ruuskanen, T. M., Rinne, J., Kajos, M. K., Hakola, H., Pohja, T., and Kulmala, M.: Technical Note: Quantitative long-term measurements of VOC concentrations by PTR-MS - measurement, calibration, and volume mixing ratio calculation methods, Atmospheric Chemistry and Physics, 8, 6681–6698, https://doi.org/10.5194/acp-8-6681-2008, https://www.atmos-chem-phys.net/8/6681/2008/, 2008.

Tsimpidi, A. P., Karydis, V. A., Zavala, M., Lei, W., Molina, L., Ulbrich, I. M., Jimenez, J. L., and Pandis, S. N.: Evaluation of the volatility basis-set approach for the simulation of organic aerosol formation in the Mexico City metropolitan area, Atmospheric Chemistry and Physics, 10, 525–546, https://doi.org/10.5194/acp-10-525-2010, https://www.atmos-chem-phys.net/10/525/2010/, 2010.

Utembe, S., Rayner, P., Silver, J., Guérette, E.-A., Fisher, J., Emmerson, K., Cope, M., Paton-Walsh, C., Griffiths, A., Duc, H., and et al.: Hot Summers: Effect of Extreme Temperatures on Ozone in Sydney, Australia, Atmosphere, 9, 466, https://doi.org/10.3390/atmos9120466, http://dx.doi.org/10.3390/atmos9120466, 2018.

van Vuuren, D. P., Edmonds, J., Kainuma, M., Riahi, K., Thomson, A., Hibbard, K., Hurtt, G. C., Kram, T., Krey, V., Lamarque, J.-F., Masui, T., Meinshausen, M., Nakicenovic, N., Smith, S. J., and Rose, S. K.: The representative concentration pathways: an overview, Climatic Change, 109, 5, https://doi.org/10.1007/s10584-011-0148-z, https://doi.org/10.1007/s10584-011-0148-z, 2011.

Yáñez-Serrano, A. M., Mahlau, L., Fasbender, L., Byron, J., Williams, J., Kreuzwieser, J., and Werner, C.: Heat stress increases the use of cytosolic pyruvate for isoprene biosynthesis, Journal of Experimental Botany, 70, 5827–5838, https://doi.org/10.1093/jxb/erz353, https://doi.org/10.1093/jxb/erz353, 2019.

Table 1. Geographic range size of each *Eucalyptus* species in Australia and the isoprene emission rate by dry leaf weight basis

Tree	Common name	Area (km^h)[a]	% weight	Emission category	Average emission $\mu g\ g^{-1}\ h^{-1}$
E. camaldulensis	River red gum	6 040 600	86.32	high	16.6[b] 28.0[c] 32.5[d]
E. tereticornis	Forest red gum	792 575	11.32	high	32.7[e] 38.2[f]
E. smithii	Blackbutt peppermint	95 750	1.37	unknown	-
E. botryoides	Bangalay	74 175	1.06	moderate	5.3[b]

[a] Species area in 2014 (from González-Orozco et al. (2016)). [b] He et al. (2000). [c]Karkik and Winer (2001) [d] Benjamin et al. (1996). [e] Nelson et al. (2000). [f] Jiang (2020), from trees growing in ambient CO_2 concentrations.

Table 2. Average isoprene basal emission rates (BER), leaf mass per unit area (LMA) and temperature at maximum γT from each pool of trees under the current and future climate growth conditions. Values in brackets are standard deviations. Data in right-hand column is derived from model fits.

Treatment	Species	No. of trees	BER, μg g^{-1} hr^{-1}	LMA, g m^{-2}	Temp at max γT, K
current climate	*E. tereticornis*	6	29.14 (13.91)	61.53 (5.42)	317.8
	E. smithii	6	41.21 (17.31)	54.93 (13.71)	317.8
	E. botryoides	6	42.46 (23.64)	72.51 (15.25)	318.4
	E. camaldulensis	6	42.87 (22.87)	72.79 (6.14)	322.1
future climate	*E. tereticornis*	6	41.57 (28.08)	64.05 (9.58)	317.3
	E. botryoides	5	55.18 (27.27)	77.96 (12.55)	317.5
	E. smithii	6	61.61 (20.01)	58.08 (5.10)	317.0
	E. camaldulensis	5	66.95 (22.44)	73.18 (4.64)	321.5

Table 3. Changes to MEGAN variables based on fitted data from current and future climate growth experiments. Percentages in brackets indicate change in maximum daily isoprene emissions due to change in variable. *Value of average LEF from the inner 3 km domain.

	MEGAN2.1	current climate growth treatment	future climate growth treatment
Average LEF (μg g^{-1} hr^{-1})	9491 *	4919 (-48%)	6585 (-31 %)
C_{T1} (kJ mol^{-1})	95	110.55 (-1 %)	75.04 (+1 %)
C_{T2} (kJ mol^{-1})	230	167.11 (+5 %)	1158.36 (-19 %)
T_{max}(K)	313	325 (-55 %)	323 (-46 %)
C_{eo}	2	6.77 (+238 %)	7.69 (+282 %)
All variables without LEF		+81 %	+76 %
All variables + LEF		-7 %	+23 %

Table 4. Description of each model experiment. CC = current climate, FC = future climate.

Experiment	Name	Emission factors	Temperature response	Meteorology used to drive MEGAN	γC
1	Base	default	default	current	x
2	CC_γT	default	fitted CC	current	x
3	CC_γT+LEF	CC LEF	fitted CC	current	x
4	FC_γT	default	fitted FC	current	x
5	FC_γT+LEF	FC LEF	fitted FC	current	x
6	Climate2050	FC LEF	fitted FC	current + δ2050	x
7	Climate2050_γC	FC LEF	fitted FC	current + δ2050	✓

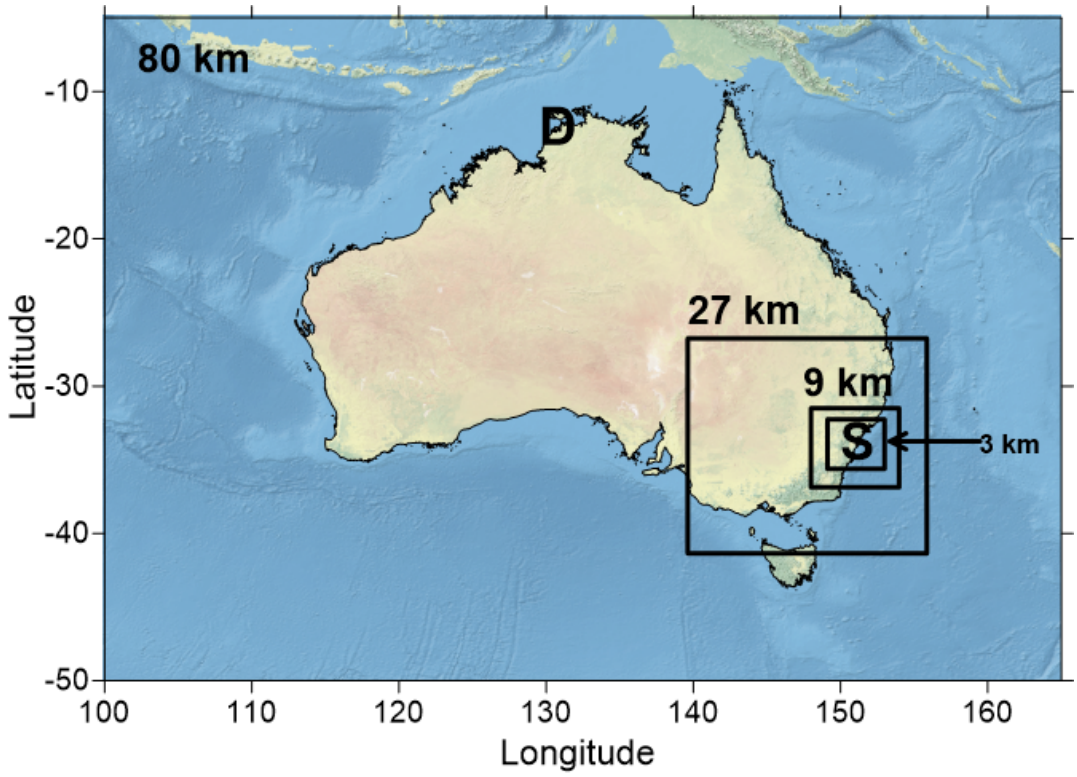

Figure 1. Map to show nests of model domains from 80 km Australia-wide to 3 km inner Sydney domain. 'S' and 'D' mark the locations of Sydney and Darwin, respectively.

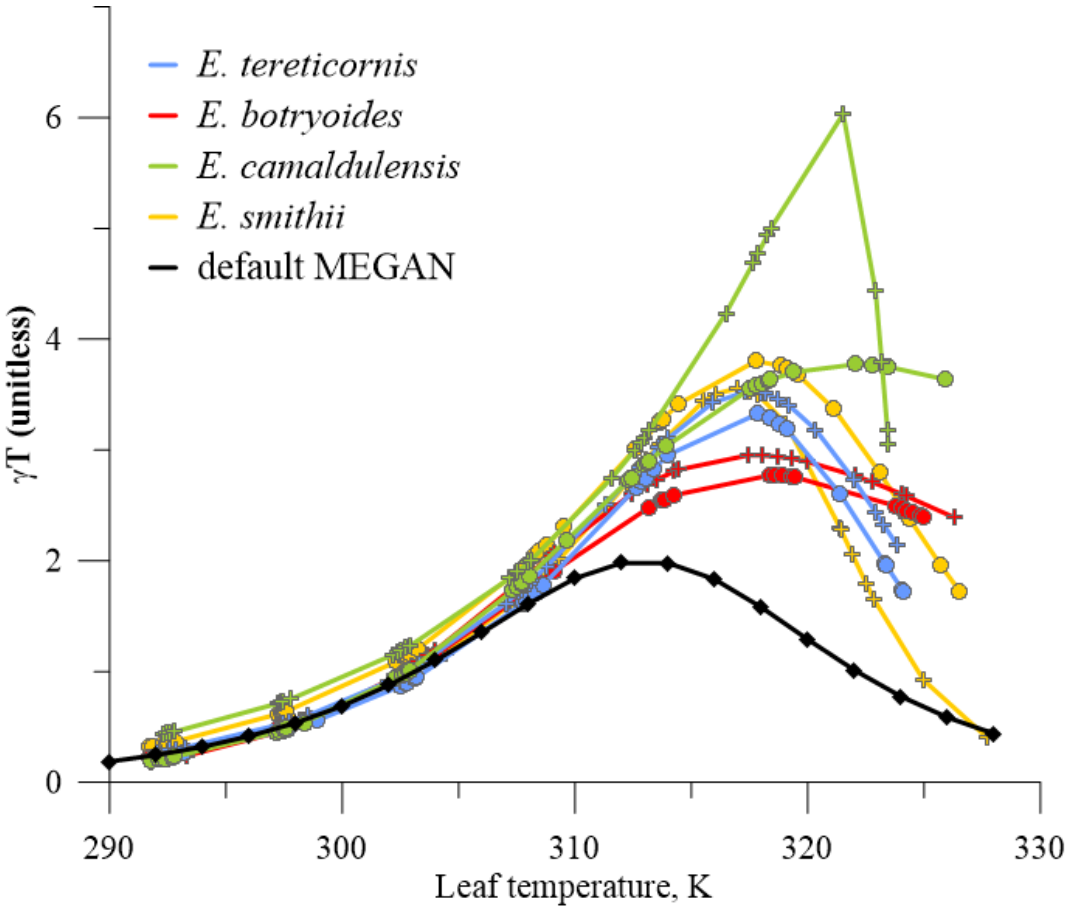

Figure 2. Comparison of γT with leaf temperature calculated using default values in MEGAN to results from four eucalypt tree species under current climate (filled circles) and future climate (+ sign) growth conditions.

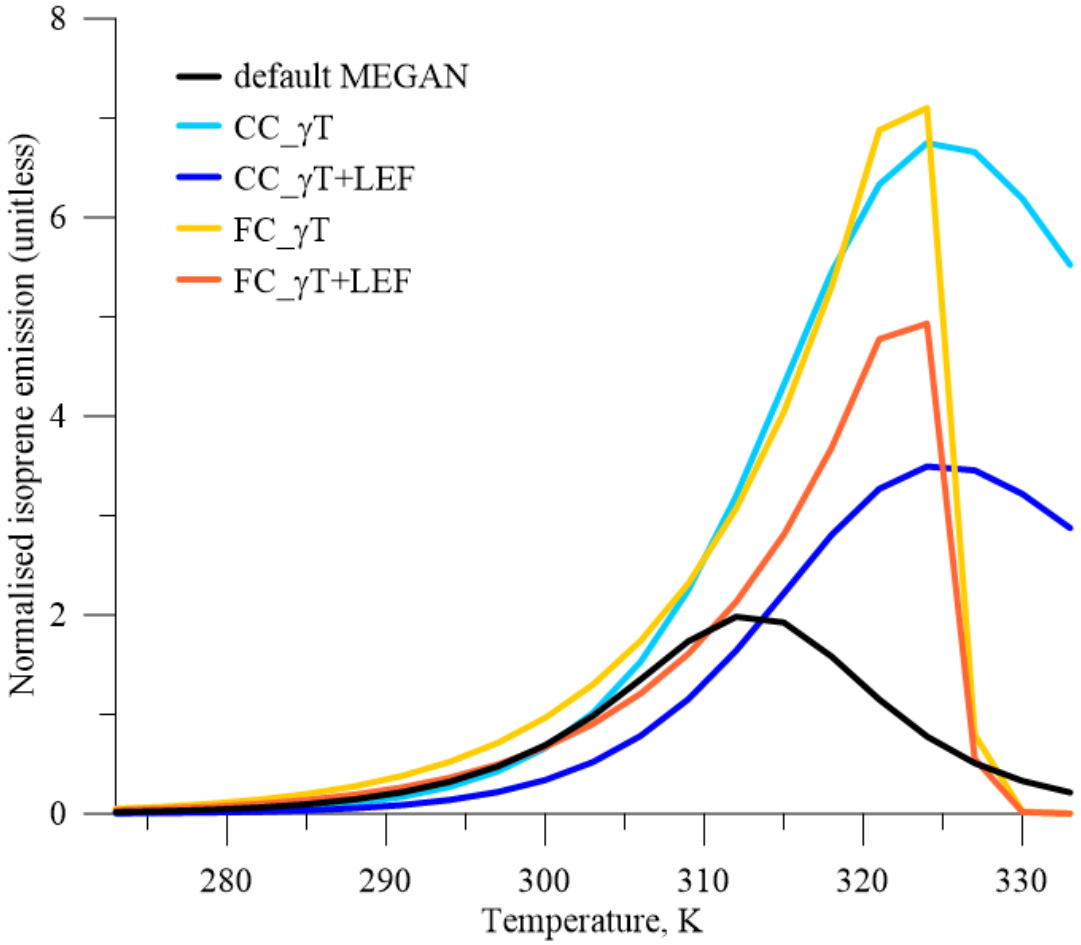

Figure 3. Impacts of new MEGAN variables on normalised isoprene emission rates at increasing ambient temperatures.

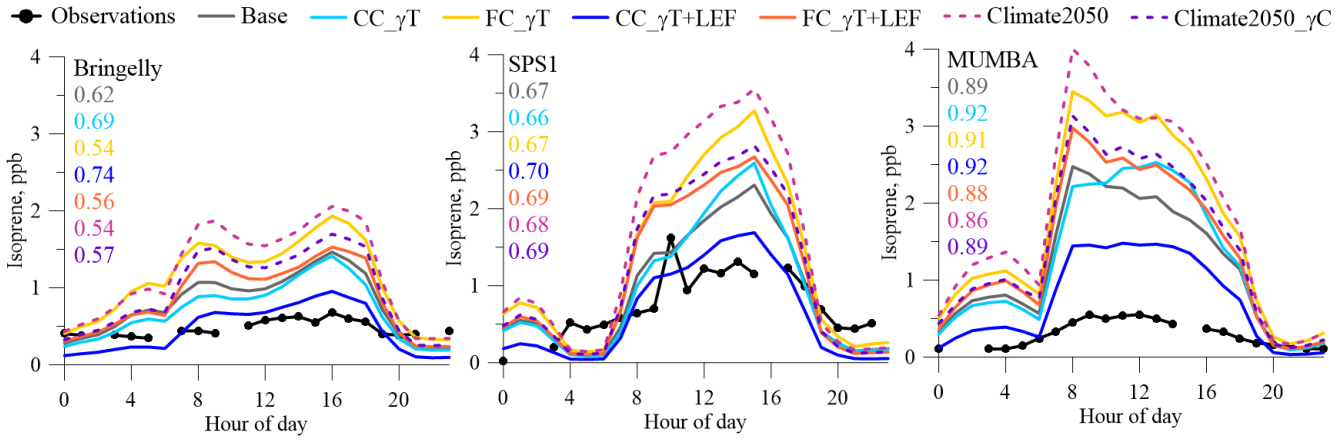

Figure 4. Average diurnal time series in isoprene mixing ratios incurred by the different model experiments at each field campaign site. r^2 values between modelled and observed isoprene given in same colours as legend.

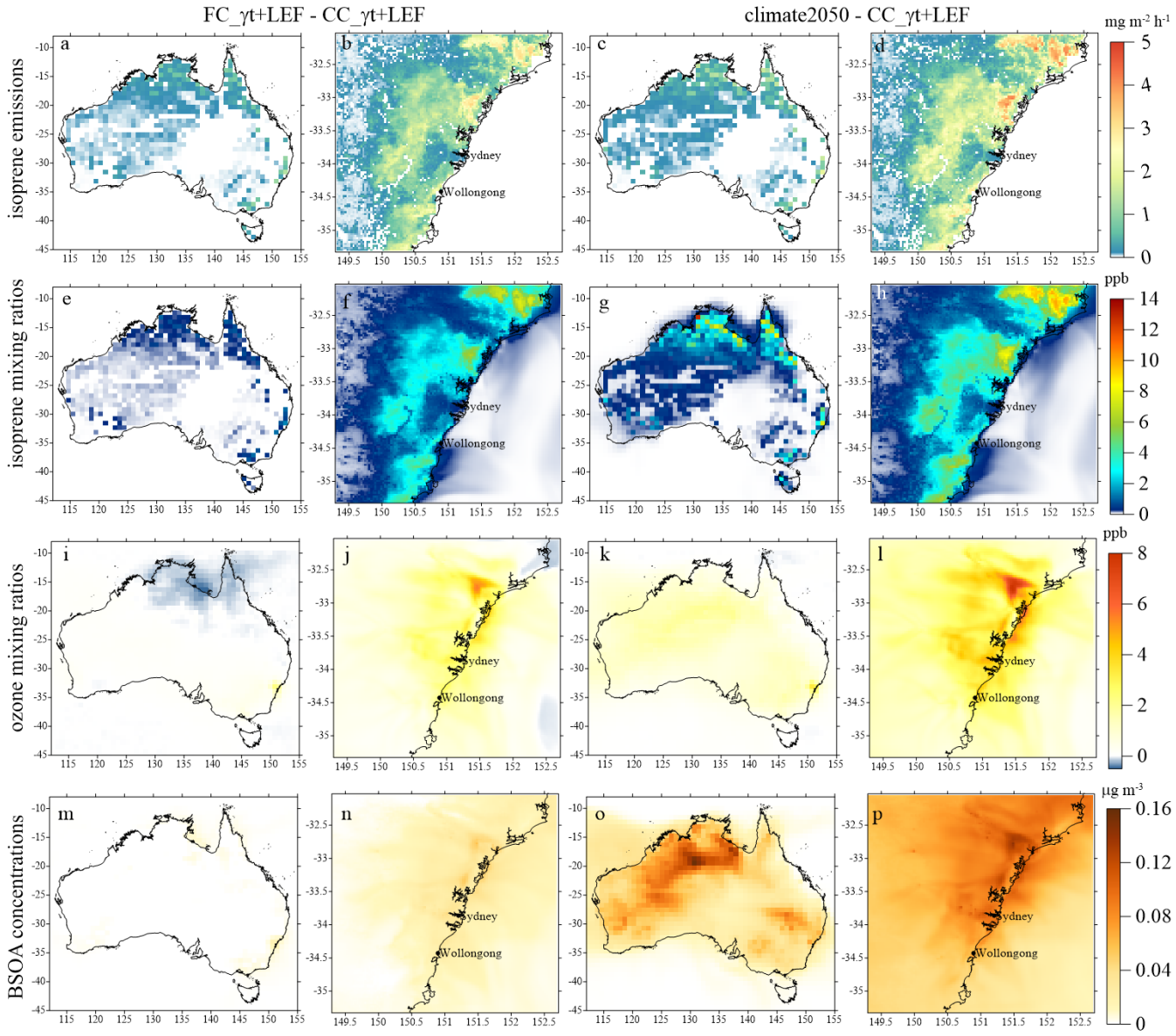

Figure 5. Difference between FC_γT+LEF and CC_γT+LEF runs (panels a, b, e, f, i, j, m and n) during the SPS1 campaign. The difference between the climate2050 runs and CC_γT+LEF runs are shown in panels c, d, g, h, k, l, o and p. Left to right, panels a-d: Isoprene emission, panels e-h: isoprene mixing ratio, panels i-l: ozone mixing ratio and panels m-p: biogenic SOA concentration in Australia at 80 km and Sydney at 3 km domains.

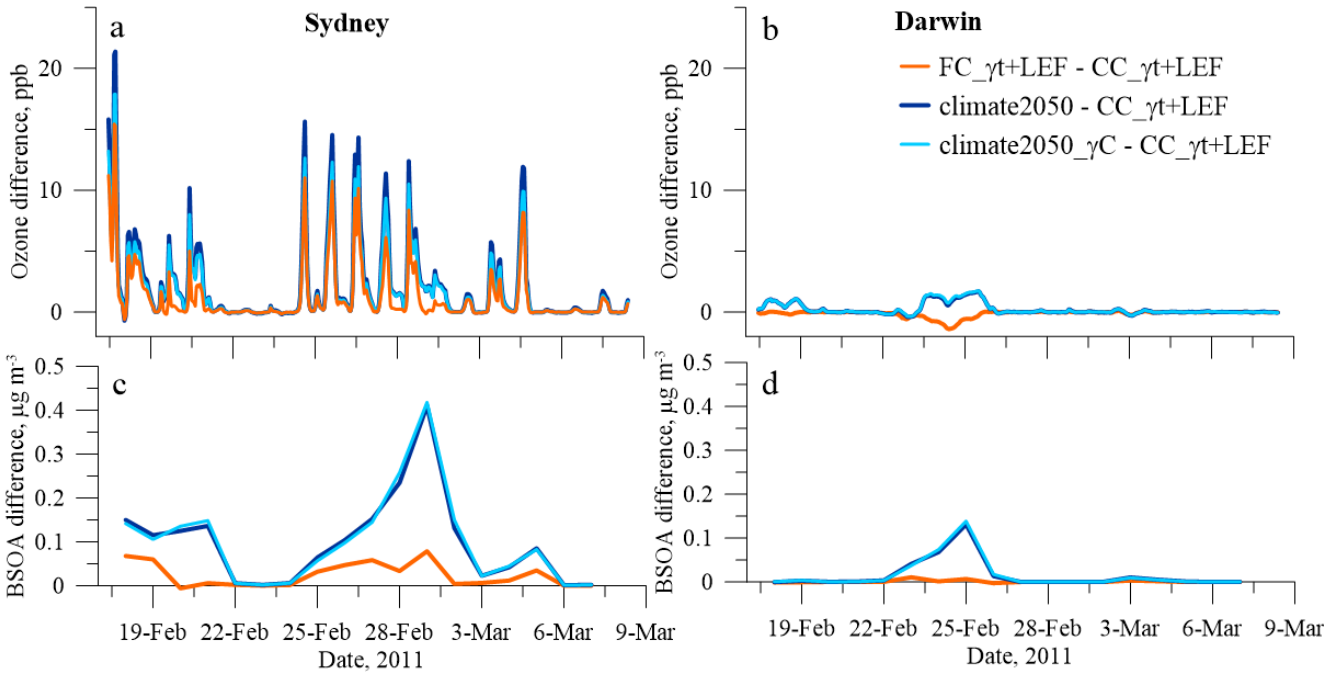

Figure 6. Differences in hourly ozone (panels a and b) and biogenic secondary organic aerosol (panels c and d) due to three 2050 experiments at Sydney and Darwin during the SPS1 campaign period.